2.1 Twisted Beam under Tip

REFERENCE	MacNeal et al.[1]
ELEMENTS	Shell elements, solid elements
MODEL FILENAME	Linearstatic01.gts

Figure 2.1.1 shows a twisted beam structure subjected to two tip forces. A fixed boundary condition is assigned to the root of the beam. A unit force is applied at the tip in two different directions. Displacements at the point the A are determined.

Figure 2.1.1
Twisted beam model

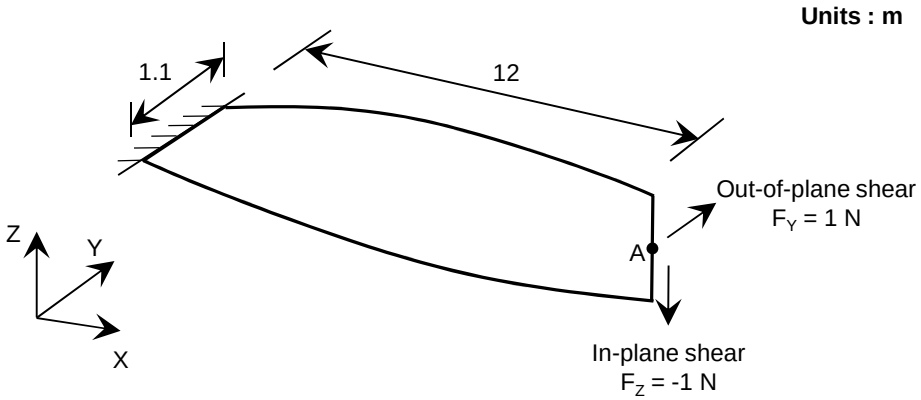

Material data	Young's modulus	*E = 29 MPa*
	Poisson's ratio	*¬ = 0.22*
Section property	Thickness	*t = 0.32 m*

Table 2.1.1 Displacements u_Y and u_Z at the point A obtained using shell elements

Load		u_Z^A [m] in-plane shear F_Z	u_Y^A [m] out-of-plane shear F_Y
Reference		*5.424ò10-3*	*1.754ò10-3*
Element type	Number of elements		
TRIA-3	2×(12×2)	*5.322ò10-3*	*1.463ò10-3*
QUAD-4	2×12	*5.405ò10-3*	*1.733ò10-3*
TRIA-6	2×(12×2)	*5.408ò10-3*	*1.752ò10-3*
QUAD-8	2×12	*5.415ò10-3*	*1.754ò10-3*

Table 2.1.2 Displacements u_Y and u_Z at the point A obtained using solid elements

Load		u_Z^A [m] in-plane shear F_Z	u_Y^A [m] out-of-plane shear F_Y
Reference		5.424×10^{-3}	*1.754×10^{-3}*
Element type	Number of elements		
TETRA-4	144	*0.384×10^{-3}*	*0.267×10^{-3}*
PENTA-6	48×1	*2.344×10^{-3}*	*0.743×10^{-3}*
HEXA-8	2×12×1	*5.411×10^{-3}*	*1.738×10^{-3}*
TETRA-10	144	*5.440×10^{-3}*	*1.767×10^{-3}*
PENTA-15	48×1	*5.367×10^{-3}*	*1.747×10^{-3}*
HEXA-20	2×12×1	*5.382×10^{-3}*	*1.752×10^{-3}*

2.2 Curved Cantilevered Beam under Tip Load

REFERENCE	MacNeal et al.[1]
ELEMENTS	Beam elements, shell elements, solid elements
MODEL FILENAME	Linearstatic02.gts

Figure 2.2.1 shows a curved beam structure subjected to tip forces in two different directions. A fixed boundary condition is assigned to the root of the beam. A unit force is applied at the free end in two different directions. Displacements at the point A are determined.

Figure 2.2.1
Curved cantilevered beam model

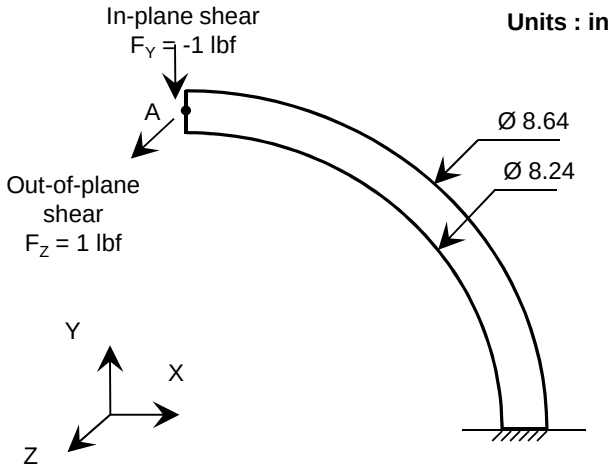

Material data	Young's modulus	*E = 10 Mpsi*
	Poisson's ratio	¬ *= 0.25*
Section property	Thickness	*t = 0.1 in*

Table 2.2.1 Displacements u_Y and u_Z at the point A obtained using beam elements

Load		u_Y^A [*in*] in-plane shear F_Y	u_Z^A [*in*] out-of-plane shear F_Z
Reference		*-8.734ò10^{-2}*	*5.022ò10^{-1}*
Element type	Number of elements		
BEAM-2	6	*-8.735x10^{-2}*	*4.968x10^{-1}*
BEAM -3	3	*-8.368x10^{-2}*	*4.864x10^{-1}*

Table 2.2.2 Displacements u_Y and u_Z at the point A obtained using shell elements

Load		u_Y^A [*in*] in-plane shear F_Y	u_Z^A [*in*] out-of-plane shear F_Z
Reference		*-8.734ò10^{-2}*	*5.022ò10^{-1}*
Element type	Number of elements		
TRIA-3	1x(6x2)	*-0.222x10^{-2}*	*4.347x10^{-1}*
QUAD-4	1x6	*-8543x10^{-2}*	*4.739x10^{-1}*
TRIA-6	1x(6x2)	*-8.756x10^{-2}*	*4.728x10^{-1}*
QUAD-8	1x6	*-8.850x10^{-2}*	*4.813x10^{-1}*

Table 2.2.3 Displacements u_Y and u_Z at the point A obtained using solid elements

Load		u_Y^A [*in*] in-plane shear F_Y	u_Z^A [*in*] out-of-plane shear F_Z
Reference		*-8.734ò10^{-2}*	*5.022ò10^{-1}*
Element type	Number of elements		
TETRA-4	76	*-0.236x10^{-2}*	*0.043x10^{-1}*
PENTA-6	1 x (6 x 2) x 1	*-0.221x10^{-2}*	*0.347x10^{-1}*
HEXA-8	1 x 6 x 1	*-8.534x10^{-2}*	*4.415x10^{-1}*
TETRA-10	76	*-8.778x10^{-2}*	*4.599x10^{-1}*
PENTA-15	1 x (6 x 2) x 1	*-8.752x10^{-2}*	*4.687x10^{-1}*
HEXA-20	1 x 6x1	*-8.848x10^{-2}*	*4.778x10^{-1}*

2.3 Cantilevered Beam under Various Tip Loads

REFERENCE	MacNeal et al.[1]
ELEMENTS	Shell elements, solid elements
MODEL FILENAME	Linearstatic03.gts

Figure 2.3.1 shows a straight beam subjected to tip forces in three different directions and twisting moment. A fixed boundary condition is assigned to the root of the beam. Unit forces and moment are applied at the free end. Displacements and twist angle at the point A are determined by using three kinds of meshes (mesh A, B and C) and using shell and solid elements. Twist angle at the point A is determined by the relative displacements of point B and C.

Figure 2.3.1
Cantilever beam model

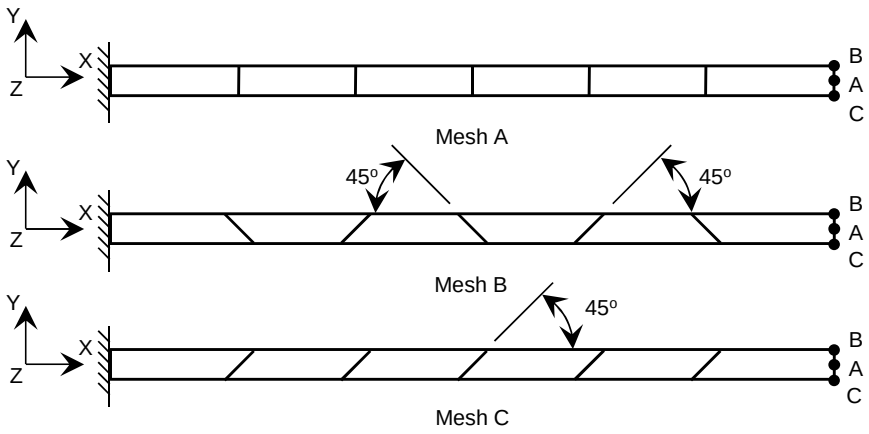

Material data	Young's modulus	*E = 10 Mpsi*
	Poisson's ratio	*¬ = 0.3*
Section property	Thickness	*t = 0.1 in*

Table 2.3.1 Displacements and rotation at the point A obtained using shell elements, mesh A

Load		u_X^A [*in*] extension F_X	u_Y^A [*in*] out-of-plane F_Y	u_Z^A [*in*] in-plane F_Z	θ_X^A [*rad*] twist M_X
Reference		*3.000ò10^{-5}*	*4.321ò10^{-1}*	*1.081ò10^{-1}*	*3.408ò10^{-2}*
Element type	Number of elements				
TRIA-3	2×(12×2)	*3.000ò10^{-5}*	*4.199x10^{-1}*	*0.034x10^{-1}*	*2.979x10^{-2}*
QUAD-4	2×12	*3.000ò10^{-5}*	*4.238x10^{-1}*	*1.073x10^{-1}*	*3.019x10^{-2}*
TRIA-6	2×(12×2)	*3.000ò10^{-5}*	*4.306x10^{-1}*	*1.074x10^{-1}*	*3.055x10^{-2}*
QUAD-8	2×12	*3.000ò10^{-5}*	*4.326x10^{-1}*	*1.081x10^{-1}*	*3.037x10^{-2}*

Table 2.3.2 Displacements and rotation at the point A obtained using shell elements, mesh B

Load		u_X^A [*in*] extension F_X	u_Y^A [*in*] out-of-plane F_Y	u_Z^A [*in*] in-plane F_Z	θ_X^A [*rad*] twist M_X
Reference		*3.000*	*4.321*	*1.081*	*3.408*
Element type	Number of elements				
TRIA-3	2×(12×2)	*3.000*	*4.177x10^{-1}*	*0.016x10^{-1}*	*3.137x10^{-2}*
QUAD-4	2×12	*3.000*	*4.171x10^{-1}*	*0.240x10^{-1}*	*3.020x10^{-2}*
TRIA-6	2×(12×2)	*3.000*	*4.297x10^{-1}*	*1.049x10^{-1}*	*3.065x10^{-2}*
QUAD-8	2×12	*3.000*	*4.331x10^{-1}*	*1.057x10^{-1}*	*3.023x10^{-2}*

Table 2.3.3 Displacements and rotation at the point A obtained using shell elements, mesh C

Load		u_X^A [*in*] extension F_X	u_Y^A [*in*] out-of-plane F_Y	u_Z^A [*in*] in-plane F_Z	θ_X^A [*rad*] twist M_X
Reference		*3.000*	*4.321*	*1.081*	*3.408*
Element type	Number of elements				
TRIA-3	2×(12×2)	*3.000*	*4.201x10^{-1}*	*0.024x10^{-1}*	*3.508x10^{-2}*
QUAD-4	2×12	*3.000*	*4.238x10^{-1}*	*0.086x10^{-1}*	*3.022x10^{-2}*
TRIA-6	2×(12×2)	*3.000*	*4.330x10^{-1}*	*1.058x10^{-1}*	*3.055x10^{-2}*
QUAD-8	2×12	*3.000*	*4.316x10^{-1}*	*1.080x10^{-1}*	*3.034x10^{-2}*

Table 2.3.4 Displacements and rotation at the point A obtained using solid elements, mesh A

Load		u_X^A [*in*] extension F_X	u_Y^A [*in*] out-of-plane F_Y	u_Z^A [*in*] in-plane F_Z	θ_X^A [*rad*] twist M_X
Reference		*3.000*	*4.321*	*1.081*	*3.408*
Element type	Number of elements				
TETRA-4	222	*3.000*	*0.031x10^{-1}*	*0.023x10^{-1}*	*0.029x10^{-2}*
PENTA-6	1x(6x2)x1	*3.000*	*0.509x10^{-1}*	*0.034x10^{-1}*	*0.077x10^{-2}*
HEXA-8	1x6x1	*3.000*	*4.249x10^{-1}*	*1.072x10^{-1}*	*2.931x10^{-2}*
TETRA-10	222	*3.000*	*3.973x10^{-1}*	*1.021x10^{-1}*	*2.883x10^{-2}*
PENTA-15	1x(6x2)x1	*3.000*	*4.301x10^{-1}*	*1.074x10^{-1}*	*2.960x10^{-2}*
HEXA-20	1x6x1	*3.000*	*4.322x10^{-1}*	*1.081x10^{-1}*	*2.935x10^{-2}*

Table 2.3.5 Displacements and rotation at the point A obtained using solid elements, mesh B

Load		u_X^A [*in*] extension F_X	u_Y^A [*in*] out-of-plane F_Y	u_Z^A [*in*] in-plane F_Z	θ_X^A [*rad*] twist M_X
Reference		*3.000*	*4.321*	*1.081*	*3.408*
Element type	Number of elements				
TETRA-4	222	*3.000*	*0.025x10^{-1}*	*0.015x10^{-1}*	*0.030x10^{-2}*
PENTA-6	1x(6x2)x1	*3.000*	*0.101x10^{-1}*	*0.016x10^{-1}*	*0.102x10^{-2}*
HEXA-8	1x6x1	*3.000*	*0.490x10^{-1}*	*0.231x10^{-1}*	*2.909x10^{-2}*
TETRA-10	222	*3.000*	*3.895x10^{-1}*	*0.998x10^{-1}*	*2.880x10^{-2}*
PENTA-15	1x(6x2)x1	*3.000*	*4.270x10^{-1}*	*1.049x10^{-1}*	*2.956x10^{-2}*
HEXA-20	1x6x1	*3.000*	*4.298x10^{-1}*	*1.057x10^{-1}*	*2.985x10^{-2}*

Table 2.3.6 Displacements and rotation at the point A obtained using solid elements, mesh C

Load		u_X^A [*in*] extension F_X	u_Y^A [*in*] out-of-plane F_Y	u_Z^A [*in*] in-plane F_Z	θ_X^A [*rad*] twist M_X
Reference		*3.000*	*4.321*	*1.081*	*3.408*
Element type	Number of elements				
TETRA-4	222	*3.000*	*0.030x10^{-1}*	*0.022x10^{-1}*	*0.035x10^{-2}*
PENTA-6	1x(6x2)x1	*3.000*	*0.149x10^{-1}*	*0.023x10^{-1}*	*0.098x10^{-2}*
HEXA-8	1x6x1	*3.000*	*2.786x10^{-1}*	*0.847x10^{-1}*	*2.931x10^{-2}*
TETRA-10	222	*3.000*	*4.052x10^{-1}*	*1.033x10^{-1}*	*2.888x10^{-2}*
PENTA-15	1x(6x2)x1	*3.000*	*4.241x10^{-1}*	*1.058x10^{-1}*	*2.966x10^{-2}*
HEXA-20	1x6x1	*3.000*	*4.318x10^{-1}*	*1.080x10^{-1}*	*2.966x10^{-2}*

2.4 Pinched Hemispherical Shell with Hole

REFERENCE	MacNeal et al.[1], Simo et al.[2]
ELEMENTS	Shell elements, solid elements
MODEL FILENAME	Linearstatic04.gts

Figure 2.4.1 shows one quadrant of a pinched hemispherical shell with inward and outward forces at the point B and point A. The hemisphere has an 18° hole at the top, and the quadrant of the hemisphere is modeled utilizing a symmetric boundary condition. Displacement at the point A is determined.

Figure 2.4.1
Pinched hemispherical shell with hole

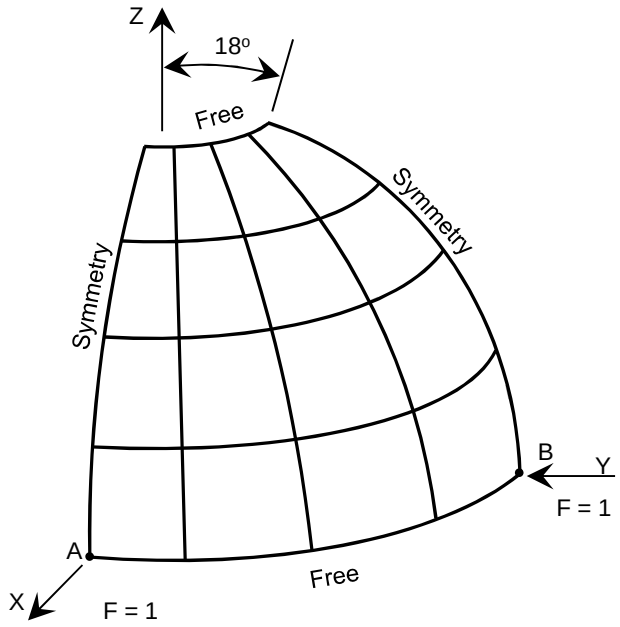

Material data	Young's modulus	$E = 6.825 \times 10^7$ *psi*
	Poisson's ratio	$\neg = 0.3$
Section property	Thickness	$t = 0.04$ *in*

Table 2.4.1 Displacement u_X at the point A obtained using shell elements

		u_X^A [in]		
Reference		*9.4x10^{-2} (Ref. 2-1), 9.3x10^{-2}(Ref. 2-2)*		
Number of elements		*4*	*8*	*12*
Element type	TRIA-3	*9.546x10^{-2}*	*9.380 x10^{-2}*	*9.311 x10^{-2}*
	QUAD-4	*9.413x10^{-2}*	*9.351 x10^{-2}*	*9.353 x10^{-2}*
	TRIA-6	*0.932x10^{-2}*	*4.039 x10^{-2}*	*7.167 x10^{-2}*
	QUAD-8	*8.073x10^{-2}*	*9.295 x10^{-2}*	*9.335 x10^{-2}*

Table 2.4.2 Displacement u_X at the point A obtained using solid elements

		u_X^A [in]		
Reference		*9.4x10^{-2} (Ref. 2-1), 9.3x10^{-2}(Ref. 2-2)*		
Number of elements		*4*	*8*	*12*
Element type	PENTA-6	*0.004 x10^{-2}*	*0.015 x10^{-2}*	*0.033 x10^{-2}*
	HEXA-8	*1.016 x10^{-2}*	*7.404 x10^{-2}*	*8.872 x10^{-2}*
	PENTA-15	*0.525 x10^{-2}*	*3.609 x10^{-2}*	*6.914 x10^{-2}*
	HEXA-20	*6.792 x10^{-2}*	*9.250 x10^{-2}*	*9.353 x10^{-2}*

2.5 Elliptic Plane Stress under Uniform Outward Pressure

REFERENCE	NAFEMS[3]
ELEMENTS	Plane stress elements, solid elements
MODEL FILENAME	Linearstatic05.gts

Figure 2.5.1 shows an elliptic plane stress problem. The plane is subjected to uniform outward normal pressure of 10MPa at the outer edge BC. A quarter of the elliptic plane is discretized with symmetric boundary conditions using coarse and fine meshes of plane stress and solid elements. Y-normal stress at the point A is obtained and compared with the reference solution given in the standard NAFEMS benchmarks.

Figure 2.5.1
Elliptic plane stress model

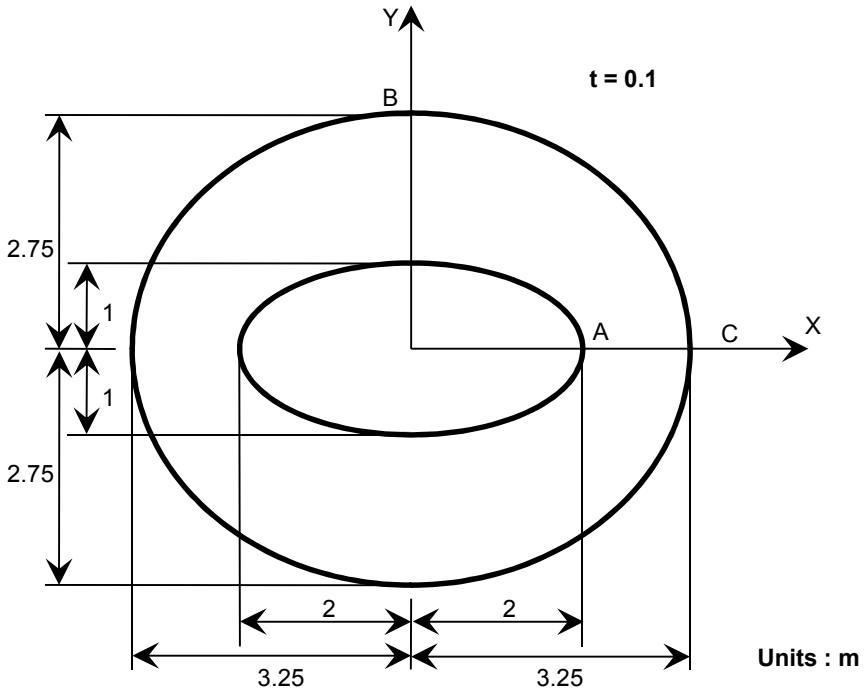

Material data	Young's modulus	*E = 210 GPa*
	Poisson's ratio	*¬ = 0.3*
Section property	Thickness	*t = 0.1 m*

Table 2.5.1 Stress $\pm_{YY}$ at the point A obtained using plane stress elements

		$\pm_{YY}^{A}$ [*MPa*]	
Reference		*92.7*	
Number of elements per side		3x2	6x4
Element type	TRIA-3	*52.9*	*72.9*
	QUAD-4	*60.9*	*80.2*
	TRIA-6	*89.3*	*93.4*
	QUAD-8	*87.1*	*92.0*

Table 2.5.2 Stress $\pm_{YY}$ at the point A obtained using solid elements

		$\pm_{YY}^{A}$ [*MPa*]	
Reference		*92.7*	
Number of elements per side		3x2	6x4
Element type	PENTA-6	*53.3*	*73.6*
	HEXA-8	*61.0*	*80.6*
	PENTA-15	*89.7*	*93.8*
	HEXA-20	*86.9*	*92.2*

2.6 Plane Truss under Concentrated Load

REFERENCE	McCormac[4]
ELEMENTS	Truss elements
MODEL FILENAME	Linearstatic06.gts

Figure 2.6.1 shows a two-dimensional truss structure consisting of different section properties. The truss structure is loaded vertically at the points A, B and C. The maximum vertical deflection which occurs at the point A is determined utilizing truss elements.

Figure 2.6.1
Truss model

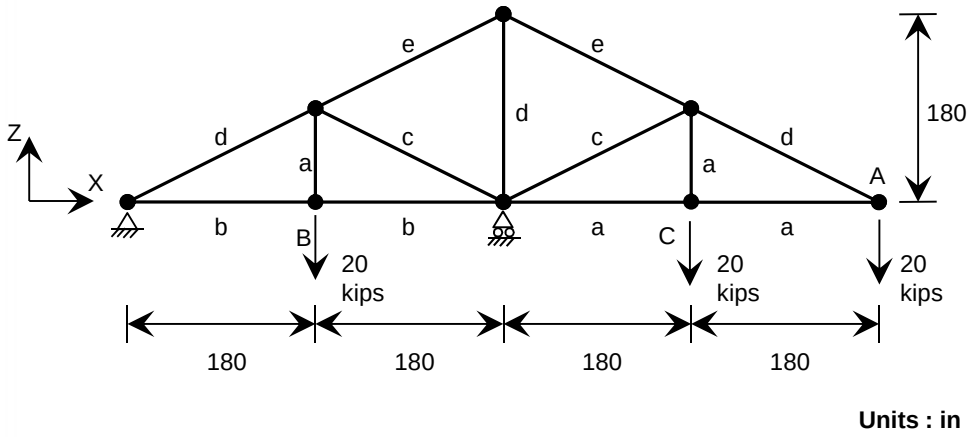

Material data	Young's modulus	$E = 3.0x10^4$ *psi*
Section property	Area	$A = 1.0\ in^2$ (element-a) $A = 2.0\ in^2$ (element-b) $A = 1.5\ in^2$ (element-c) $A = 3.0\ in^2$ (element-d) $A = 4.0\ in^2$ (element-e)

Table 2.6.1 Displacement u_Z at the point A obtained using truss elements

		u_Z^A [*in*]
Reference		*-2.63*
TRUSS-2	13-elements	*-2.63*

2.7 Skewed Plate under Uniform Pressure

REFERENCE	NAFEMS[3]
KEYWORDS	Shell elements, solid elements
MODEL FILENAME	Linearstatic07.gts

A skewed plate model with obtuse angles of 150 degrees (see Figure 2.7.1) subjected to uniform pressure of 700 Pa is evaluated. The maximum principal stress on the lower surface at the center of the plate (point E) is obtained using shell and solid elements. The reference value is taken from the standard NAFEMS benchmarks.

Figure 2.7.1
Skewed plate model

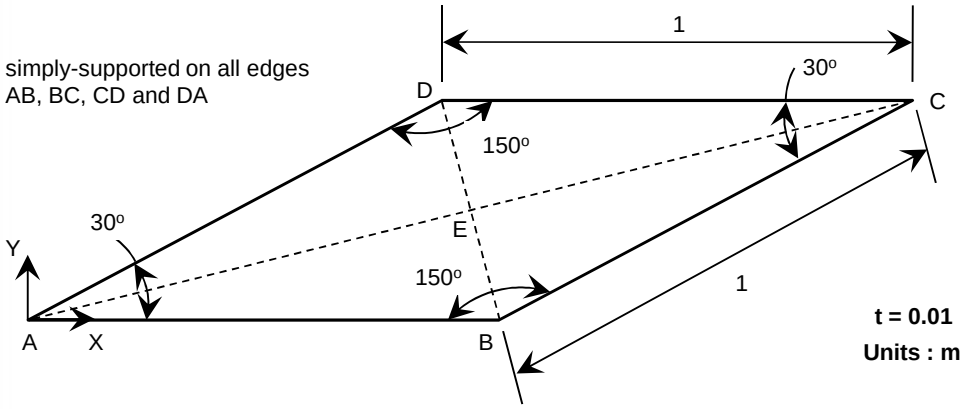

Material data	Young's modulus	*E = 210 GPa*
	Poisson's ratio	¬ *= 0.3*
Section property	Thickness	*t = 0.01 m*

Table 2.7.1 Maximum principal stress at bottom surface $\pm_{P1}$ *obtained using shell elements*

		$\pm^{E}_{P1}$ [*MPa*]		
Reference		*0.802*		
Number of elements per side		2	4	8
Element type	TRIA-3	*0.804*	*0.783*	*0.804*
	QUAD-4	*0.666*	*0.799*	*0.799*
	TRIA-6	*1.146*	*0.898*	*0.835*
	QUAD-8	*0.668*	*0.771*	*0.763*

Table 2.7.2 Maximum principal stress at bottom surface $\pm_{P1}$ obtained using solid elements

		$\pm_{P1}^{E}$ [*MPa*]		
Reference		*0.802*		
Number of elements per side		2	4	8
Element type	PENTA-6	*0.329*	*0.087*	*0.251*
	HEXA-8	*0.336*	*0.675*	*0.736*
	PENTA-15	*0.581*	*0.769*	*0.792*
	HEXA-20	*0.539*	*0.736*	*0.723*

2.8 Thick Plate under Uniform Pressure

REFERENCE	NAFEMS[3]
ELEMENTS	Shell elements, solid elements
MODEL FILENAME	Linearstatic08.gts

Figure 2.8.1 shows a thick plate clamped on the middle surface, subjected to uniform pressure of 1MPa applied on the top surface. Utilizing the symmetry, a quarter of the plate is modeled using solid elements. The normal stress ($\pm\sigma_{YY}^{D}$) at the point D is evaluated. The reference solution is taken from the NAFEMS standard benchmarks.

Figure 2.8.1
Thick plate model

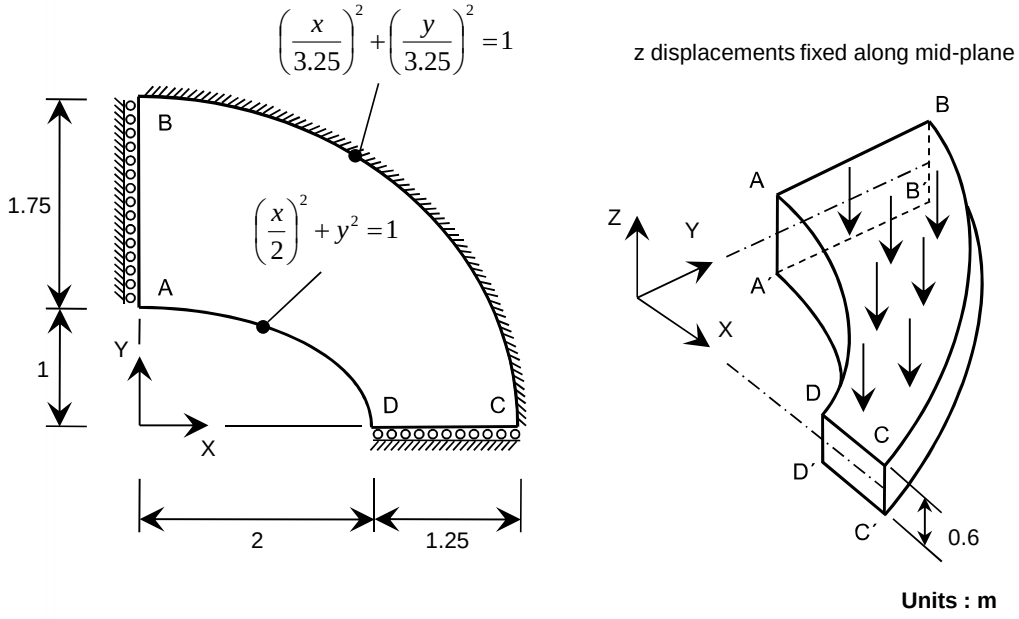

Material data	Young's modulus	*E = 210 GPa*
	Poisson's ratio	*¬ = 0.3*
Section property	Thickness	*t = 0.6 m*

Table 2.8.1 Stress $\pm_{YY}$ at the point D obtained using solid elements

		$\pm_{YY}^{D}$ [*MPa*]	
Reference		*5.38*	
Number of elements per side		3x2	6x4
Element type	PENTA-6	*4.878*	*5.751*
	HEXA-8	*5.321*	*5.577*
	PENTA-15	*6.131*	*6.039*
	HEXA-20	*5.422*	*5.062*

2.9 Cantilever with Variable Thickness

REFERENCE	Young et al[5]
ELEMENTS	Beam elements, shell elements, solid elements
MODEL FILENAME	Linearstatic09.gts

A cantilever model with thickness that varies linearly along the length is shown in Figure 2.9.1. The cantilever is subjected to either an end moment or tension. The root of the cantilever is fixed. For the end moment load, the vertical displacement at the point A is determined. For the tension load, the longitudinal displacement at the point A is determined. The cantilever is modeled using beam, shell with variable thickness and solid elements.

Figure 2.9.1
Cantilever model with variable thickness

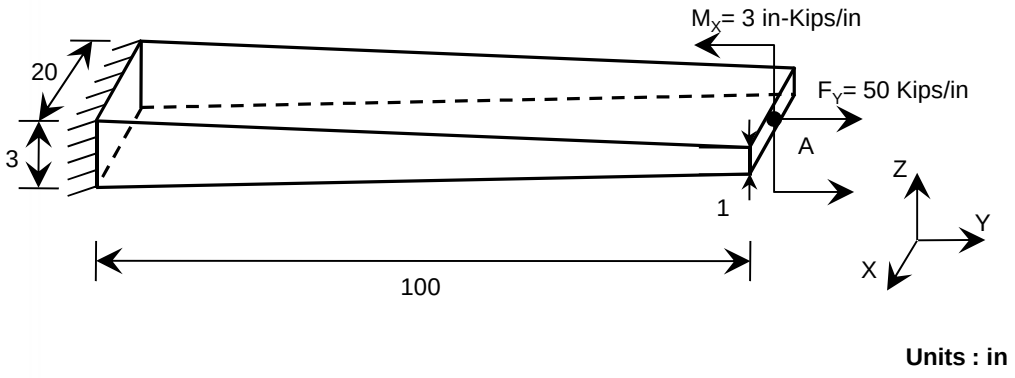

Material data	Young's modulus	*E = 1.0x10³ ksi*
	Poisson's ratio	¬ *= 0.3*

Table 2.9.1 Displacement u_Z subjected to end moment, and u_Y subjected to end tension at the point A obtained using beam elements

Load		u_Z^A [*in*] End moment	u_Y^A [*in*] End tension
Reference		*20.0*	*2.7465*
Element type	Number of elements		
BEAM-2	1	*20*	*2.7465*
BEAM-3	1	*21.5026*	*2.7273*

Table 2.9.2 Displacement u_Z subjected to end moment, and u_Y subjected to end tension at the point A obtained using shell elements

Load		u_Z^A [*in*] End moment	u_Y^A [*in*] End tension
Reference		*20.0*	*2.7465*
Element type	Number of elements		
TRIA-3	(5×2)	*19.00*	*2.6924*
QUAD-4	5	*19.98*	*2.7252*
TRIA-6	(5×2)	*19.28*	*2.7096*
QUAD-8	5	*20.07*	*2.7363*

Table 2.9.3 Displacement u_Z subjected to end moment, and u_Y subjected to end tension at the point A obtained using solid elements

Load		u_Z^A [*in*] End moment	u_Y^A [*in*] End tension
Reference		*20.0*	*2.7465*
Element type	Number of elements		
TETRA-4	60	*0.27*	*2.6930*
PYRAM-5	30	*0.50*	*2.6931*
PENTA-6	(5x3)x1	*6.09*	*2.7031*
HEXA-8	5x1	*19.95*	*2.7026*
TETRA-10	60	*19.67*	*2.7292*
PYRAM-13	30	*18.95*	*2.7380*
PENTA-15	(5x2)x1	*19.79*	*2.7351*
HEXA-20	5x1	*19.97*	*2.7356*

2.10 Scordellis-Lo Barrel Vault

REFERENCE	MacNeal[1], Simo et al.[2]
ELEMENTS	Shell elements, solid elements
MODEL FILENAME	Linearstatic10.gts

Figure 2.10.1 shows the Scordelis-Lo roof problem in which a short cylindrical shell section is subjected to a gravity force of 360 lbf/ft^3. Utilizing the symmetric boundary condition, a quarter of the cylinder is modeled with shell and solid elements. The vertical displacement at the mid-point of the free edge at the point A is determined with meshes with different refinement levels. The reference value of -0.3024 is taken for comparison.

Figure 2.10.1
Scordellis-Lo barrel vault model

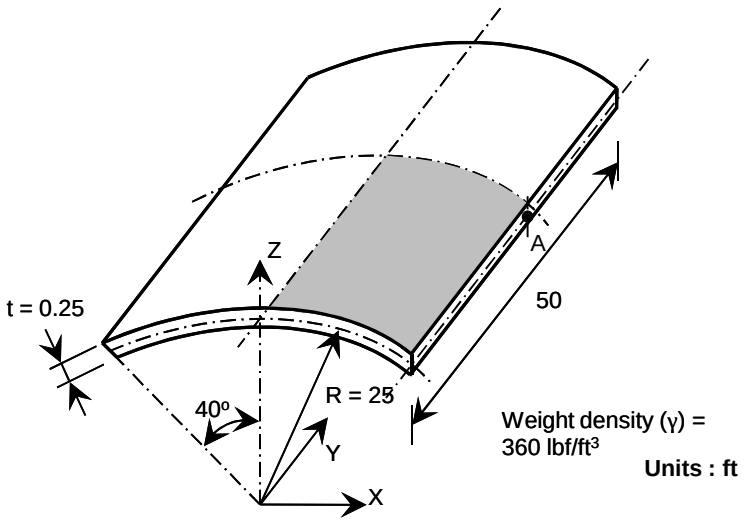

Material data	Young's modulus	$E = 4.32x10^8$ lbf/ft^2
	Poisson's ratio	¬ = 0

Table 2.10.1 Vertical displacement u_Z at the point A obtained using shell elements

		u_Z^A [*ft*]		
Reference		*-0.3024*		
Number of elements per side		*4*	*6*	*8*
Element type	TRIA-3	*-0.2019*	*-0.2381*	*-0.2603*
	QUAD-4	*-03195*	*-0.3080*	*-0.3058*
	TRIA-6	*-0.2793*	*-0.2958*	*-0.2995*
	QUAD-8	*-0.3002*	*-0.3006*	*-0.3007*

Table 2.10.2 Vertical displacement u_Z at the point A obtained using solid elements

		u_Z^A [*ft*]		
Reference		*-0.3024*		
Number of elements per side		*4*	*6*	*8*
Element type	PENTA-6	*-0.0163*	*-0.0228*	*-0.1326*
	HEXA-8	*-0.3118*	*-0.3061*	*-0.3046*
	PENTA-15	*-0.2548*	*-0.2870*	*-0.2962*
	HEXA-20	*-0.3014*	*-0.3013*	*-0.3013*

2.11 Z-section Cantilever

REFERENCE	NAFEMS[3]
ELEMENTS	Shell elements, solid elements
MODEL FILENAME	Linearstatic11.gts

Figure 2.11.1 shows a Z-section cantilever clamped on one end. A torque moment of 1.2 MN m is applied to the opposite end by a uniformly distributed edge shear force, S = 0.6 MN at each flange. The cantilever model is discretized using shell and solid elements. The axial stress is evaluated at the point A, which is compared with the reference NAFEMS benchmarks.

Figure 2.11.1
Z-section cantilever model

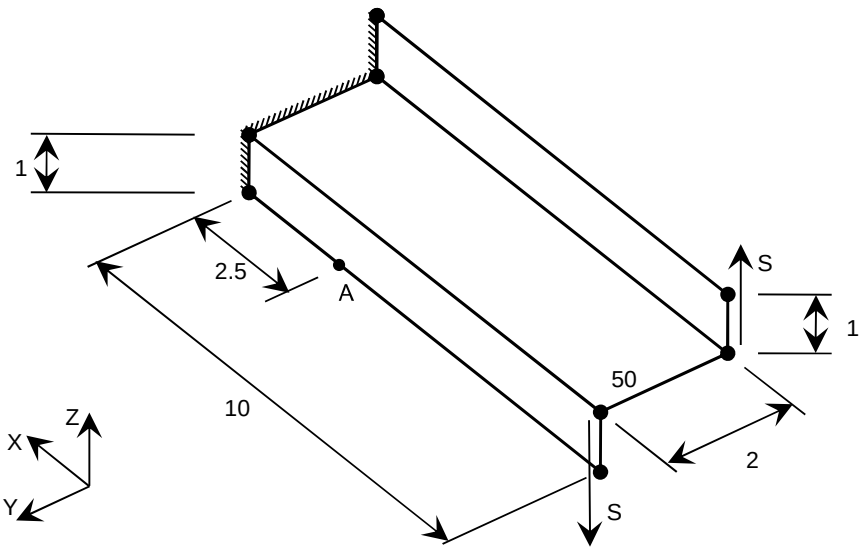

Units : m

Material data	Young's modulus	*E = 210 GPa*
	Poisson's ratio	*¬ = 0.3*
Section property	Thickness	*t = 0.1 m*

Table 2.11.1 Stress $\pm_{XX}$ at the point A obtained using shell elements

		$\pm^{A}_{XX}$ [*MPa*]
Reference		*-108*
Element type	Number of elements	
TRIA-3	48	*-30.789*
QUAD-4	24	*-110.231*
TRIA-6	48	*-107.756*
QUAD-8	24	*-110.093*

Table 2.11.2 Stress $\pm_{XX}$ at the point A obtained using solid elements

		$\pm^{A}_{XX}$ [*MPa*]
Reference		*-108*
Element type	Number of elements	
PENTA-6	48	*3.047*
HEXA-8	24	*107.357*
PENTA-15	48	*104.509*
HEXA-20	24	*107.094*

2.12 Thick Cylinder Subjected to Internal Pressure Load

REFERENCE	Young et al[5]
ELEMENTS	Plane strain elements, axisymmetric elements
MODEL FILENAME	Linearstatic12_planestrain.gts, Linearstatic12_axisymmetirc.gts

A thick infinite cylinder subjected to internal pressure of 100 MPa applied to the inner surface of the cylinder is shown in Figure 2.12.1. The model is formulated as a plane problem and an axisymmetric problem. The circumferential stress at the inner surface as well as the radial displacements at the inner and the outer surfaces are evaluated.

Figure 2.12.1
Thick cylinder model

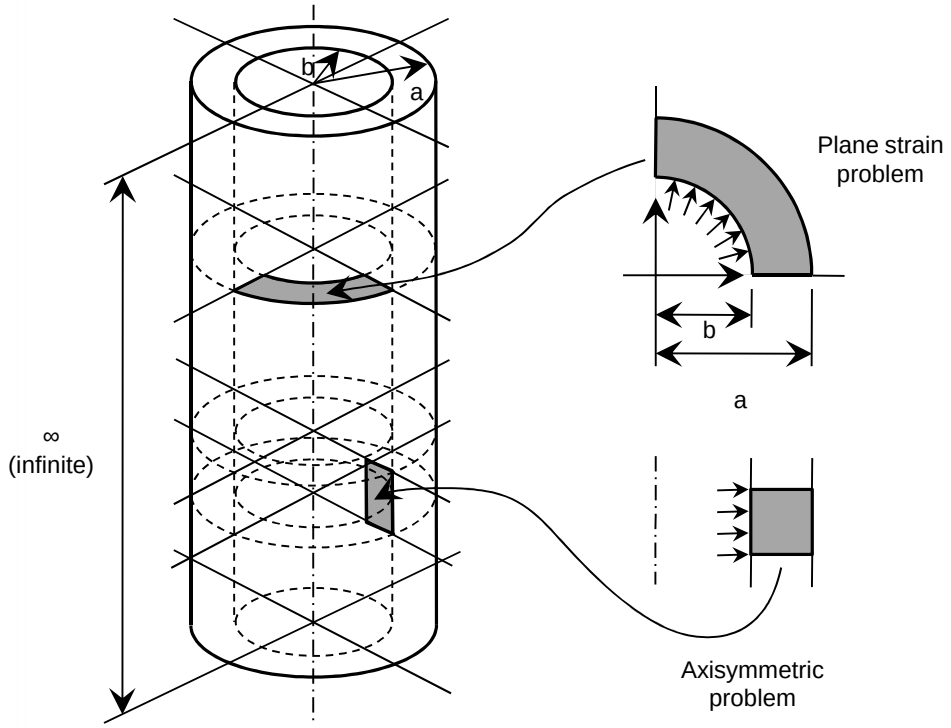

Material data	Young's modulus	*E = 220 Gpa*
	Poisson's ratio	¬ *= 0*
Section property	Major radius	*a = 0.2 m*
	Minor radius	*b = 0.1 m*

Table 2.12.1 Radial displacement u_R at inner and outer surfaces and maximum circumferential stress $\pm^{max}$ obtained using plane strain elements

		u_R [m]		$\pm^{max}$ [MPa]
		Inner surface	Outer surface	
Reference		7.936x10^{-5}	6.349x10^{-5}	166.667
Element type	Number of elements			
TRIA-3	90	7.791x10^{-5}	6.300x10^{-5}	164.506
	360	7.917 x10^{-5}	6.337x10^{-5}	165.881
QUAD-4	45	7.911x10^{-5}	6.336x10^{-5}	162.944
	180	7.930 x10^{-5}	6.346 x10^{-5}	165.659
TRIA-6	90	7.902x10^{-5}	6.332x10^{-5}	165.199
	360	7.929 x10^{-5}	6.345 x10^{-5}	166.742
QUAD-8	45	7.902x10^{-5}	6.336x10^{-5}	166.062
	180	7.936x10^{-5}	6.349 x10^{-5}	166.467

Table 2.12.2 Radial displacement u_R at inner and outer surfaces and maximum circumferential stress $\pm^{max}$ obtained using axisymmetric elements

		u_R [m]		$\pm^{max}$ [MPa]
		Inner surface	Outer surface	
Reference		7.936x10^{-5}	6.349x10^{-5}	166.667
Element type	Number of elements			
TRIAX-3	10	7.879 x10^{-5}	6.345 x10^{-5}	164.949
	20	7.920 x10^{-5}	6.348 x10^{-5}	166.185
QUADX-4	5	7.936 x10^{-5}	6.349 x10^{-5}	144.444
	10	7.936 x10^{-5}	6.349 x10^{-5}	154.545
TRIAX-6	10	7.934 x10^{-5}	6.349 x10^{-5}	165.270
	20	7.936 x10^{-5}	6.349 x10^{-5}	166.274
QUADX-8	5	7.937 x10^{-5}	6.349 x10^{-5}	164.714
	10	7.937 x10^{-5}	6.349 x10^{-5}	166.100

2.13 Hemisphere under Point Loads

REFERENCE	NAFEM[3]
ELEMENTS	Shell elements, solid elements
MODEL FILENAME	Linearstatic13.gts

Figure 2.13.1 shows a quadrant of a hemispheric shell with inward and outward forces at the point A and point B. Utilizing the symmetric condition, the quadrant model is discretized using shell and solid elements. The radial displacement at the point A is determined. The reference solution is taken from the standard NAFEMS benchmarks.

Figure 2.13.1
Hemisphere quadrant model

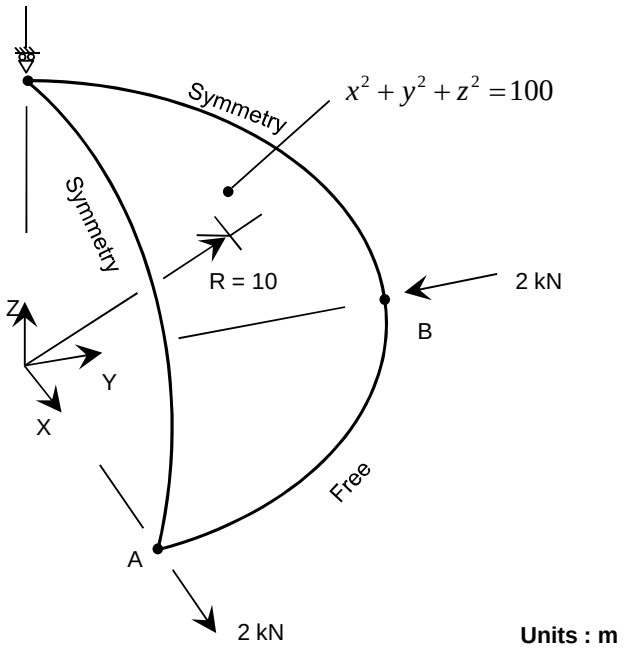

Material data	Young's modulus	*E = 68.25 Gpa*
	Poisson's ratio	¬ *= 0.3*
Section property	Thickness	*t = 0.04 m*

Table 2.13.1 Displacement u_X at the point A obtained using shell elements

		u_X^A [m]	
Reference		$1.850x10^{-1}$	
Number of elements per side		4	8
Element type	TRIA-3	$1.844\ x10^{-1}$	$1.851\ x10^{-1}$
	QUAD-4	$1.048x10^{-1}$	$1.809\ x10^{-1}$
	TRIA-6	$0.132\ x10^{-2}$	$0.703\ x10^{-2}$
	QUAD-8	$1.480x10^{-1}$	$1.832\ x10^{-1}$

Table 2.13.2 Displacement u_X at the point A obtained using solid elements

		u_X^A [m]	
Reference		$1.850x10^{-1}$	
Number of elements per side		4	8
Element type	PENTA-6	$9.422x10^{-5}$	$3.533x10^{-4}$
	HEXA-8	$9.995x10^{-3}$	$1.192x10^{-1}$
	PENTA-15	$7.702x10^{-3}$	$0.621x10^{-1}$
	HEXA-20	$1.234x10^{-1}$	$1.818x10^{-1}$

2.14 Thick/Thin Square Plates

REFERENCE	Zienkiewicz et al[6]
ELEMENTS	Shell elements, solid elements
MODEL FILENAME	Linearstatic14_thick.gts, Linearstatic14_thin.gts

Figure 2.14.1 shows a square plate with 1m in side length. All the edges are clamped. Uniform pressure of 1 Pa is applied. Two configurations are considered. Model A has a thickness of 0.1m, and Model B has a thickness of 0.001m. Utilizing the symmetric condition, a quarter of the plate is discretized using shell and solid elements. The maximum vertical displacement at the center of the plate (point A) is determined for both models.

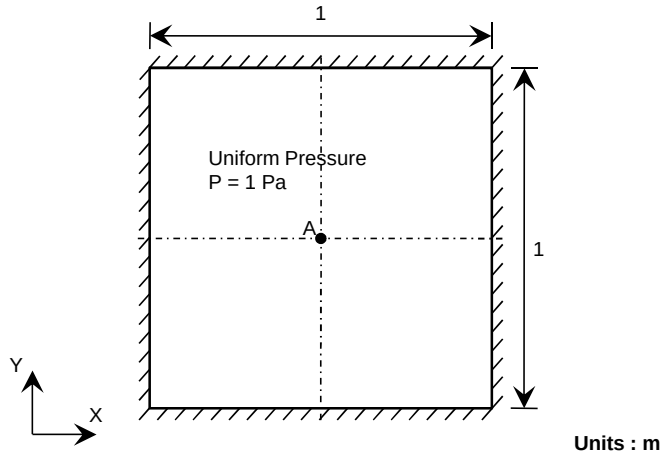

Figure 2.14.1 Hemisphere quadrant model

Material data	Young's modulus	*E = 29.0 kPa (Model A)* *E = 29.0 GPa (Model B)*
	Poisson's ratio	¬ *= 0.3*
Section property	Thickness	*t = 0.1 m (Model A)* *t = 0.001 m (Model B)*

Table 2.14.1 Displacement u_Z obtained at the point A using shell elements, t=0.1m (Model A)

		u_Z^A [m]		
Reference		*5.645x10^{-4}*		
Number of elements		*2x2*	*4x4*	*8x8*
Element type	TRIA-3	*5.548x10^{-4}*	*5.675x10^{-4}*	*5.670x10^{-4}*
	QUAD-4	*6.145x10^{-4}*	*5.815x10^{-4}*	*5.704x10^{-4}*
	TRIA-6	*6.646x10^{-4}*	*5.882x10^{-4}*	*5.722x10^{-4}*
	QUAD-8	*6.370x10^{-4}*	*6.107x10^{-4}*	*5.869x10^{-4}*

Table 2.14.2 Displacement u_Z obtained at the point A using solid elements, t=0.1m (Model A)

		u_Z^A [m]		
Reference		$5.645x10^{-4}$		
Number of elements		2x2x1	4x4x1	8x8x1
Element type	PENTA-6	$2.752x10^{-4}$	$4.358x10^{-4}$	$5.169x10^{-4}$
	HEXA-8	$5.355x10^{-4}$	$5.488x10^{-4}$	$5.516x10^{-4}$
	PENTA-15	$4.966x10^{-4}$	$5.234x10^{-4}$	$5.358x10^{-4}$
	HEXA-20	$5.010x10^{-4}$	$5.233x10^{-4}$	$5.355x10^{-4}$

Table 2.14.3 Displacement u_Z obtained at the point A using shell elements, t=0.001m (Model B)

		u_Z^A [m]		
Reference		$4.763x10^{-4}$		
Number of elements		2x2	4x4	8x8
Element type	TRIA-3	$4.533x10^{-4}$	$4.725x10^{-4}$	$4.759x10^{-4}$
	QUAD-4	$4.562x10^{-4}$	$4.714x10^{-4}$	$4.765x10^{-4}$
	TRIA-6	$4.587x10^{-4}$	$4.817x10^{-4}$	$4.792x10^{-4}$
	QUAD-8	$4.769x10^{-4}$	$4.767x10^{-4}$	$4.765x10^{-4}$

Table 2.14.4 Displacement u_Z obtained at the point A using solid elements, t=0.001m (Model B)

		u_Z^A [m]		
Reference		$4.763x10^{-4}$		
Finite element mesh		2x2x1	4x4x1	8x8x1
Element type	PENTA-6	$0.005x10^{-5}$	$0.021x10^{-5}$	$0.080x10^{-5}$
	HEXA-8	$4.667x10^{-4}$	$4.735x10^{-4}$	$4.757x10^{-4}$
	PENTA-15	$0.307x10^{-5}$	$1.517x10^{-4}$	$4.035x10^{-4}$
	HEXA-20	$1.213x10^{-4}$	$2.863x10^{-4}$	$4.606x10^{-4}$

2.15 Cylindrical Shell Patch Test

REFERENCE	NAFEMS[3]
ELEMENTS	Shell elements
MODEL FILENAME	Linearstatic15.gts

Figure 2.15.1 shows the geometry of a model. Two loading conditions are considered. In Case 1, the shell is subjected to a uniform moment of 1 kN m/m applied on the edge DC. In Case 2, the shell is subjected to uniform outward normal pressure of 0.6 MPa. The outer surface tangential stress at the point E is determined, which is compared with the reference value of 60 MPa.

Figure 2.15.1
Cylindrical shell patch test

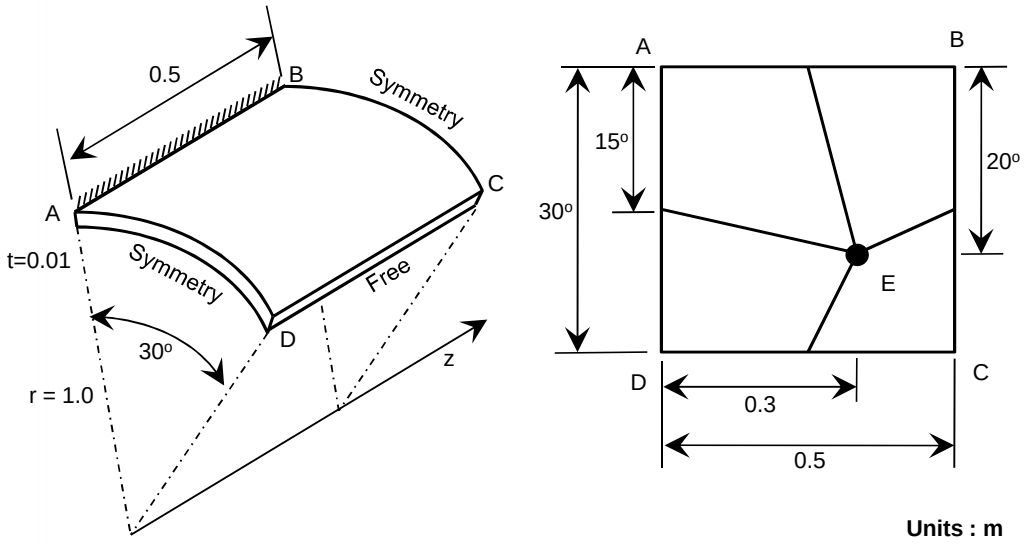

Material data	Young's modulus	*E = 210 Gpa*
	Poisson's ratio	*¬ = 0.3*
Section property	Thickness	*t = 0.01 m*

Table 2.15.1 Tangential stress ±— at the point E obtained using shell elements for load cases 1 and 2

		±^{E} [*MPa*]	
Reference		*60*	
Load Case		Edge moment (Case 1)	Outward pressure (Case 2)
Element type	Number of elements		
TRIA-3	(4x2)	*43.903*	*41.083*
QUAD-4	4	*52.908*	*68.487*
TRIA-6	(4x2)	*35.749*	*60.093*
QUAD-8	4	*51.865*	*56.637*

2.16 Axisymmetric Shell under Pressure

REFERENCE	NAFEMS[3]
ELEMENTS	Axisymmetric elements
MODEL FILENAME	Linearstatic16.gts

Figure 2.16.1 shows an axisymmetric shell structure subjected to uniform normal pressure. The points A and E are constrained in the vertical and radial directions respectively. The hoop stress on the outer surface at the point D is determined using a coarse mesh and a fine mesh. The reference solution is taken from the standard NAFEMS benchmarks.

Figure 2.16.1
Axisymmetric shell model

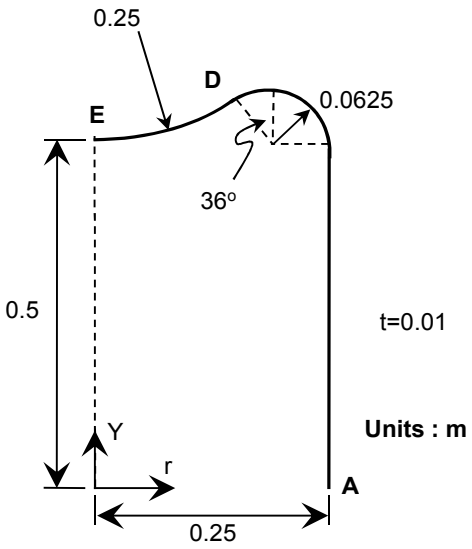

Material data	Young's modulus	*E = 210 Gpa*
	Poisson's ratio	*¬ = 0.3*

Table 2.16.1 Tangential stress ±— at the point D obtained using axisymmetric elements

		±^{D} [*MPa*]
Reference		*94.55*
Element type	Number of elements	
TRIA-3	(4x21)x1	*55.61*
	(4x42)x2	*71.93*
QUAD-4	21x1	*66.59*
	42x2	*78.41*
TRIA-6	(4x21)x1	*88.78*
	(4x42)x2	*90.05*
QUAD-8	21x1	*88.84*
	42x2	*90.08*

2.17 Stresses Caused by a Point Load

REFERENCE	Boussinesq[7]
ELEMENTS	Axisymmetric elements
MODEL FILENAME	Linearstatic17.gts

Boussinesq presented the following solution for vertical stresses with a semi-infinite soil subjected to a vertical point load applied at the surface.

$$\Delta\pm_z = \frac{3P}{2®}\frac{z^3}{(r^2+z^2)^{5/2}}$$

The solution is based on the assumption that soil is semi-infinite, homogeneous, linearly elastic and isotropic. Figure 2.17.1 shows the semi-infinite soil model as an axisymmetric structure constrained in radial direction and clamped at the bottom. A vertical point load, $P = 10kN$, is applied at the origin of coordinate system. The vertical stresses along the vertical direction at r=0.05 obtained using axisymmetric elements are compared with the Boussinesq solution.

Figure 2.17.1
Semi-infinite soil model with axisymmetric elements

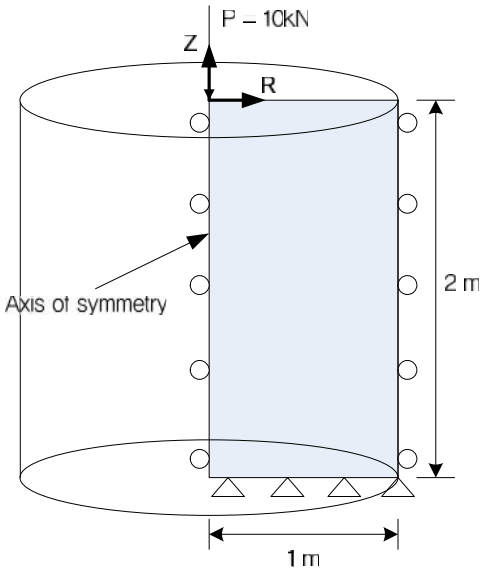

Material data	Young's modulus	*E = 10 Gpa*
	Poisson's ratio	*¬ = 0.3*

Figure 2.17.2
Comparison stresses with Boussinesq solution

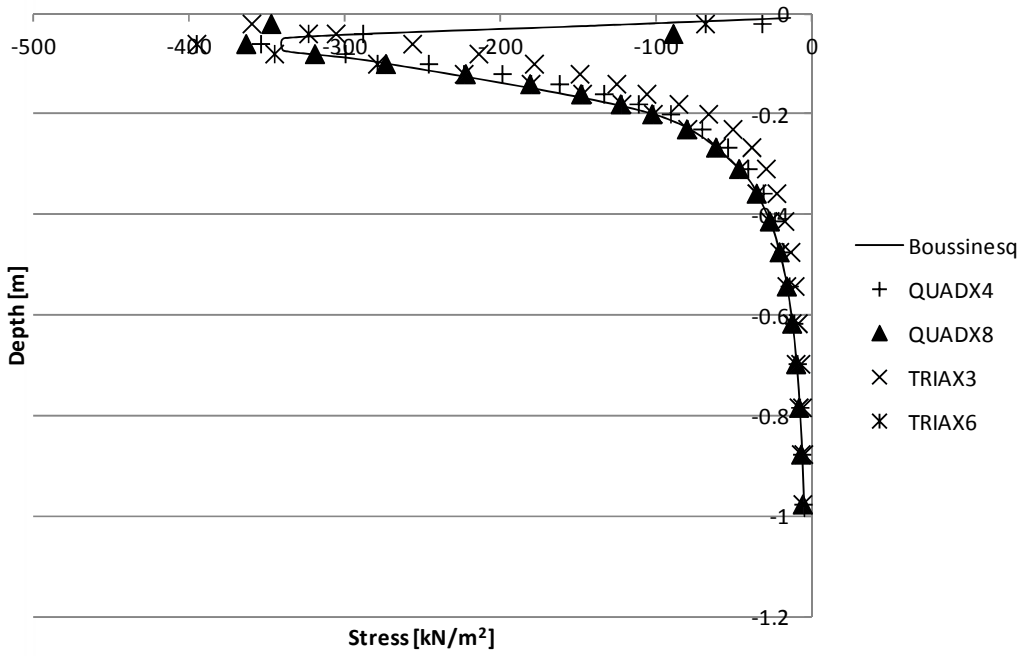

2.18 Stresses Caused by a Line Load

REFERENCE	Boussinesq[7]
ELEMENTS	Plane strain elements
MODEL FILENAME	Linearstatic18.gts

A line uniform line load is applied along the y-axis at the surface of a soil structure. The resulting stress is independent of y and plane strain elements are employed to solve the problem. Figure 2.18.1 shows the problem as a plane strain soil model. A line load, $q = 10kN/m$ is applied at the origin of coordinate system. The bottom surface is clamped and the left and right surfaces are constrained in the x direction. Linear static analysis is carried out to obtain the vertical stress along the z-direction at x=0. An analytical solution by Bonssinesq is taken for comparison.

$$\Delta\pm_z = \frac{2qz^3}{\circledR(x^2+z^2)^2}$$

Figure 2.18.1
Soil model with plane strain elements

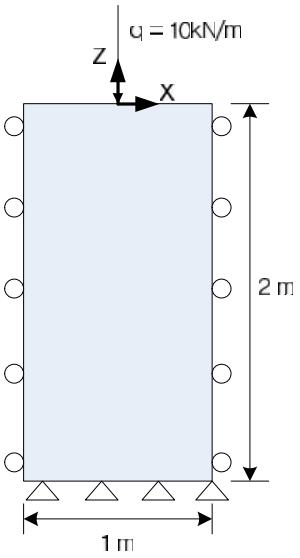

Material data	Young's modulus	*E = 10 Gpa*
	Poisson's ratio	*¬ = 0.3*

Figure 2.18.2
Comparison stresses with Boussinesq solution

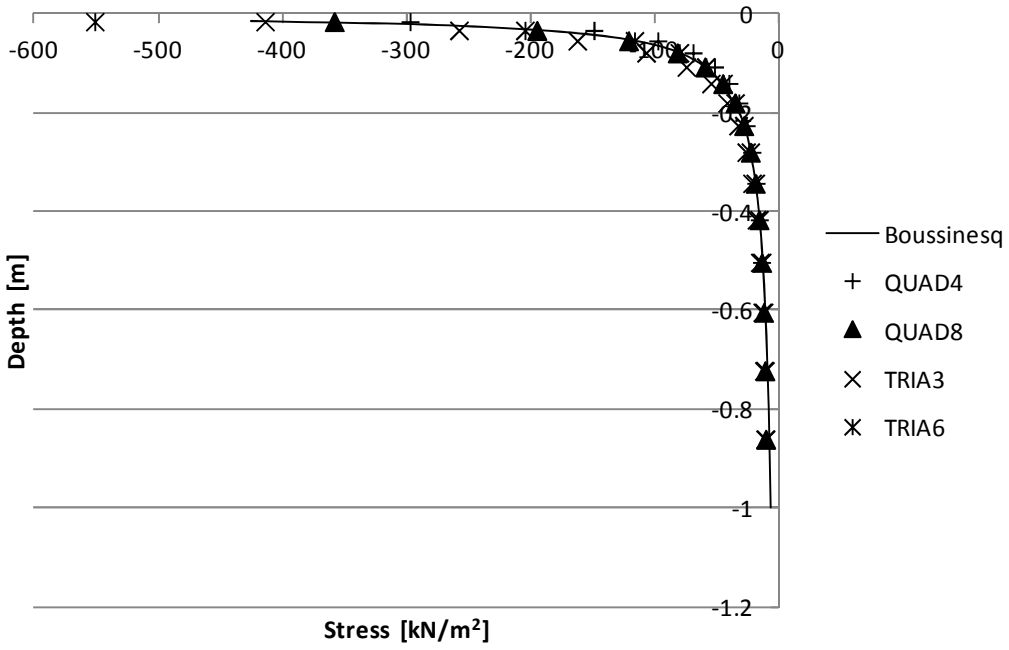

2.19 Stresses Caused by a Circular Load

REFERENCE	Boussinesq[7]
ELEMENTS	Axisymmetric elements
MODEL FILENAME	Linearstatic19.gts

Figure 2.19.1 shows an axisymmetric soil constrained in the radial direction and clamped at the bottom. A uniform pressure of $q = 10\,kPa$ is applied on a circular area with radius R on the top surface. Vertical stresses at the center of the loaded area are obtained using axisymmetric elements. Comparison is made with an analytical solution given by Boussinesq in the following form:

$$\Delta\pm_z = q\left\{1 - \frac{1}{\left[(R/z)^2 + 1\right]^{3/2}}\right\}$$

Figure 2.19.1
Semi-infinite soil model with axisymmetric elements

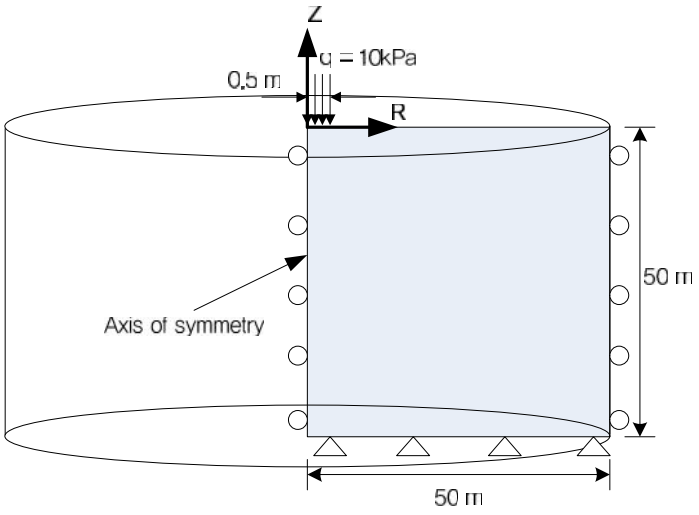

Material data	Young's modulus	*E = 10 Gpa*
	Poisson's ratio	*¬ = 0.3*

Figure 2.19.2
Comparison stresses with Boussinesq solution

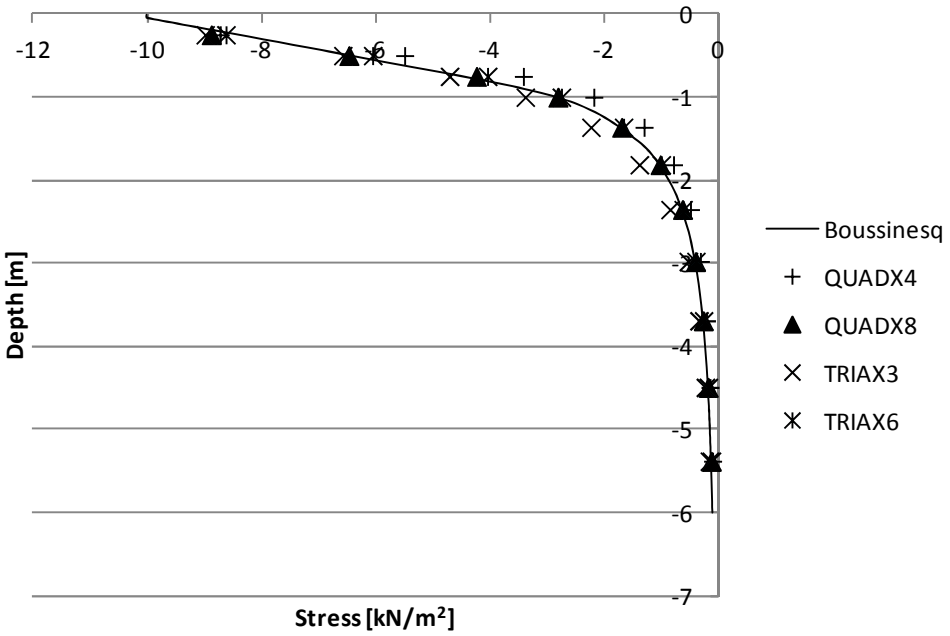

2.20 Stresses Caused by a Strip Load

REFERENCE	Boussinesq[7]
ELEMENTS	Plane strain elements
MODEL FILENAME	Linearstatic20.gts

Plane strain elements are employed to solve the stresses caused by a uniformly distributed strip load. As depicted in Figure 2.20.1, the plane strain soil model is constrained in x direction and clamped at bottom. Taking into account the symmetry of the problem, only half of problem is modeled.

Pressure, $q = 10kPa$ is applied on a strip with width, $B = 1m$ at the origin of coordinate system. The vertical stresses at $x = 0.25m$ are compared with an analytical solution by Boussinesq:

$$\Delta\pm_z = \frac{q}{\pi}\left\{\tan^{-1}\left(\frac{x}{z}\right) - \tan^{-1}\left(\frac{x-B}{z}\right) + \sin\left[\tan^{-1}\left(\frac{x}{z}\right) - \tan^{-1}\left(\frac{x-B}{z}\right)\right]\cos\left[\tan^{-1}\left(\frac{x}{z}\right) + \tan^{-1}\left(\frac{x-B}{z}\right)\right]\right\}$$

where q is the applied pressure and B is the width of strip load.

Figure 2.20.1
Soil model with plane strain elements

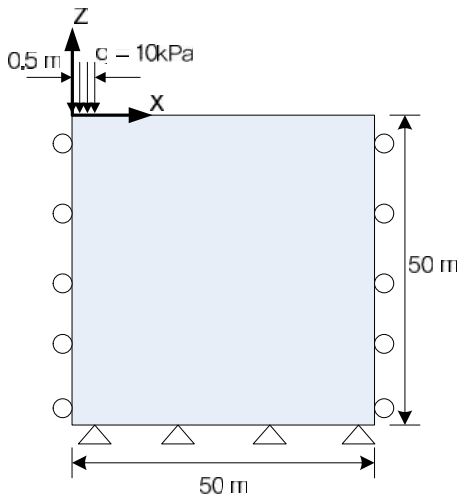

Material data	Young's modulus	*E = 10 Gpa*
	Poisson's ratio	*¬ = 0.3*

Figure 2.20.2
Comparison stresses with Boussinesq solution

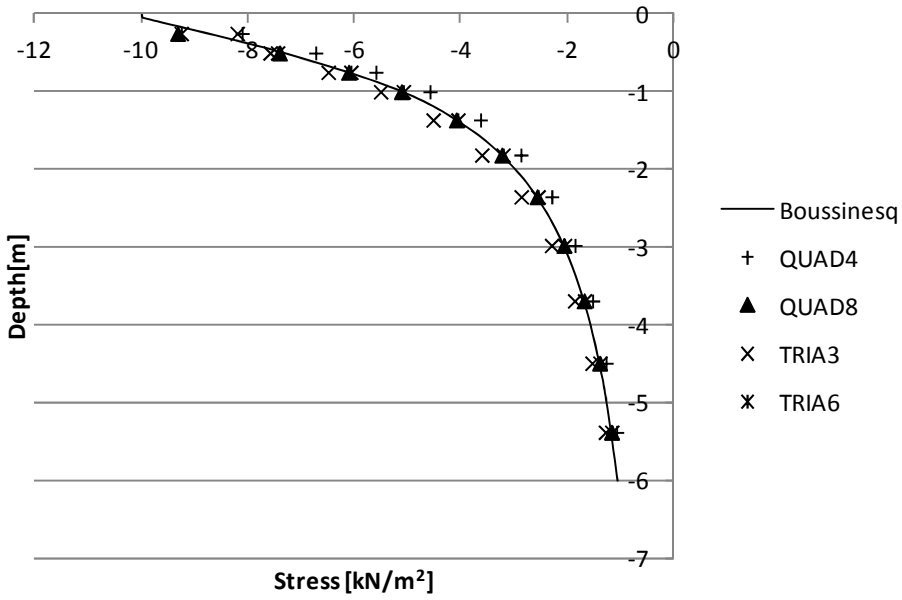

2.21 Stress in Soil with Hydrostatic Pressure

REFERENCE	Das[8]
ELEMENTS	Plane strain, solid, axisymmetric elements
MODEL FILENAME	Linearstatic21.gts

Figure 2.21.1 shows soil subjected to hydrostatic pore pressure and self-weight. Two cases are considered with different water level. In case (A), the water level is above the upper surface of the model and in case (B), the water level is below the upper surface of the model. Linear static analysis is carried out with plane strain, solid and axisymmetric elements to obtain vertical stress along the vertical axis. Partially saturated effects are not considered and the stress and pore pressure relations are based on the Terzaghi's effective stress principle. The total and effective vertical stresses are compared with analytical solution (Figure 2.21.2). The analytical solution for total and effective vertical stresses can be represented as:

Case A:

$$\pm_y(y) = -h_f ¥_f - (H-y)¥_{sat}$$
$$\pm_y'(y) = -(H-y)(¥_{sat} - ¥_f)$$

Case B:

$$\pm_y(y) = \begin{cases} -h_f' ¥_{unsat} - (H - h_f' - y)¥_{sat} & (0 \le y < H - h_f') \\ -(H-y)¥_{unsat} & (H - h_f' \le y \le H) \end{cases}$$
$$\pm_y'(y) = \begin{cases} -h_f' ¥_{unsat} - (H - h_f' - y)(¥_{sat} - ¥_f) & (0 \le y < H - h_f') \\ -(H-y)¥_{unsat} & (H - h_f' \le y \le H) \end{cases}$$

Figure 2.21.1
Soil model with different water levels

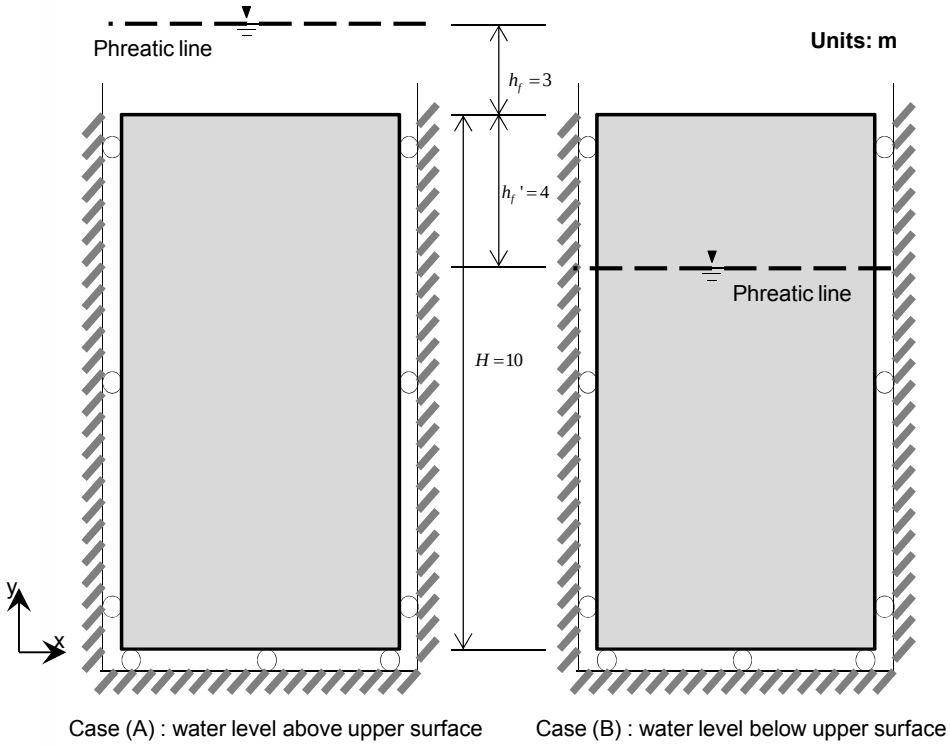

Material data	Young's modulus	*E = 100 kPa*
	Poisson's ratio	¬ *= 0.3*
Weight densities	Water	$¥_f = 9.80665\,kN/m^3$
	Saturated soil	$¥_{sat} = 25\,kN/m^3$
	Unsaturated soil	$¥_{unsat} = 17\,kN/m^3$

Total and effective vertical stress distributions obtained using plane strain elements compared with analytical solutions

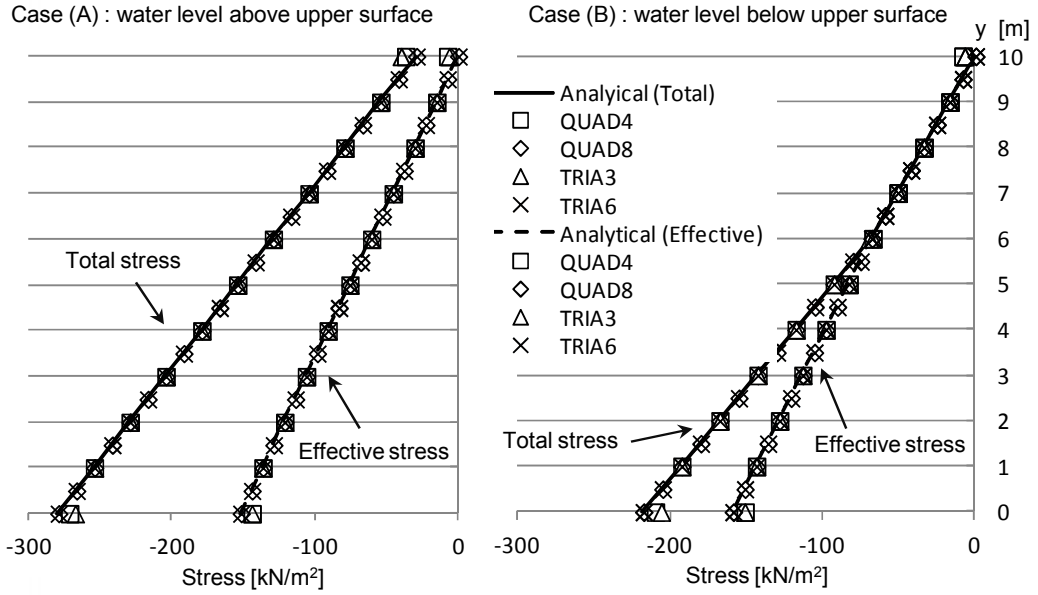

Total and effective vertical stress distributions obtained using solid elements compared with analytical solutions

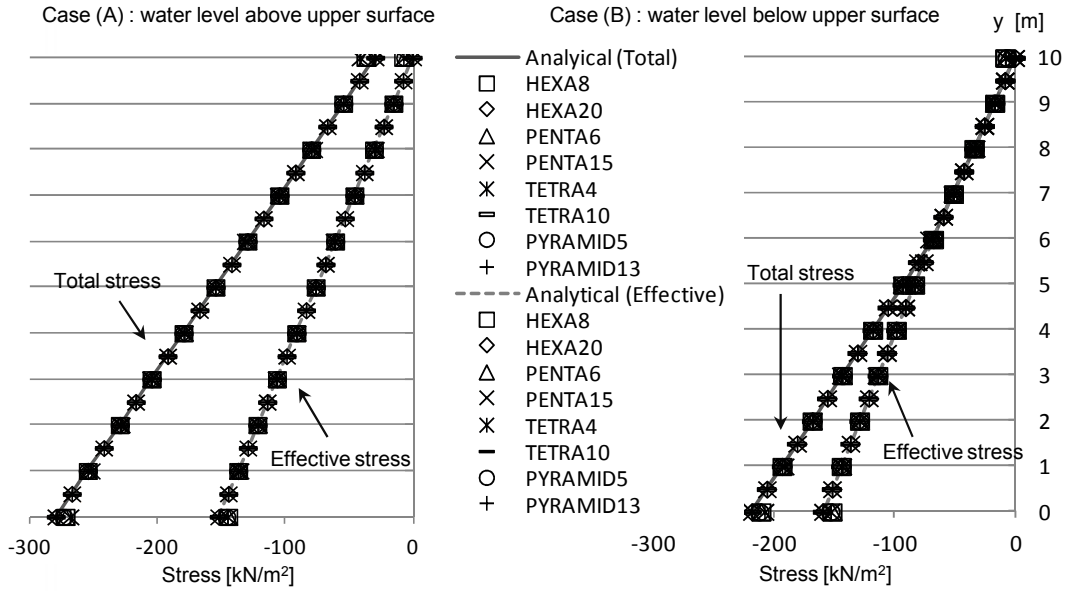

Total and effective vertical stress distributions obtained using axisymmetric elements compared with analytical solutions

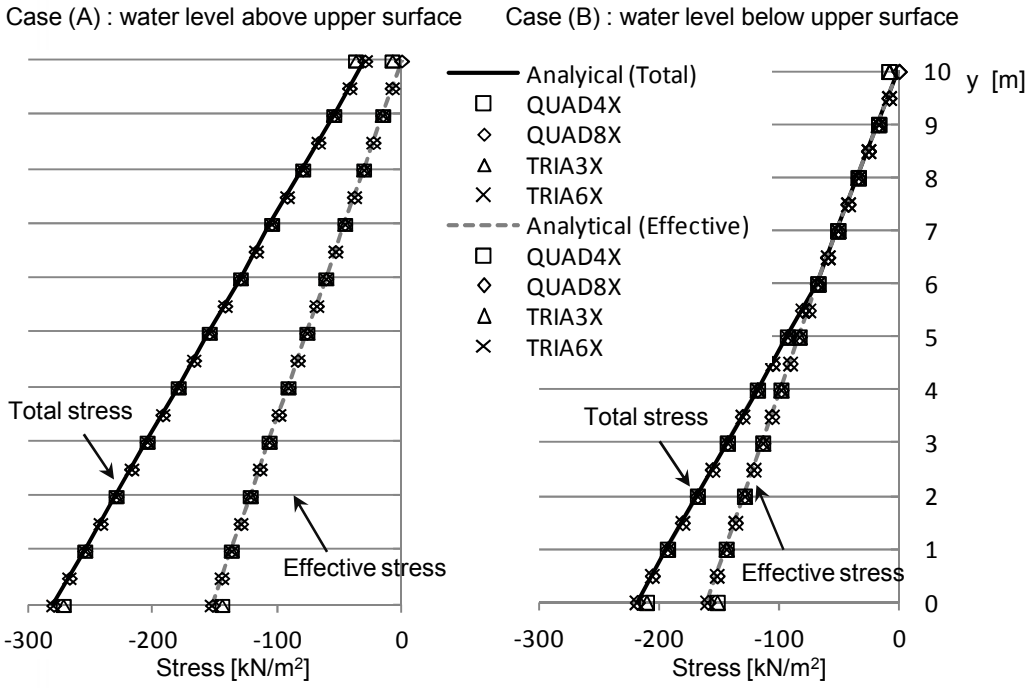

2.22 Stress in Partially Saturated Soil

REFERENCE	Das[8]
ELEMENTS	Plane strain, solid, axisymmetric elements
MODEL FILENAME	Linearstatic22.gts

Figure 2.22.1 shows soil subjected to hydrostatic pore pressure and self-weight. Linear stress analysis is carried out considering partially saturated effects on stress and specific weight. Therefore Bishop's effective stress relation is utilized. Effective saturation is assumed to be equal to 1 for positive pore pressure and vary linearly with negative pore pressure up to $p = -¥_f h_c$ where saturation is zero (see Figure 2.22.2). Total and effective vertical stresses can be obtained analytically in the following form:

$$\pm_y(y) = \begin{cases} -(H - h_f^{'} - y)¥_{sat} - h_f^{'}\ ¥_{unsat} - \dfrac{h_c}{2}(¥_{sat} - ¥_{unsat}) & \left(0 \le y \le H - h_f^{'}\right) \\ -\left\{-h_f^{'} + \dfrac{h_c}{2} + \dfrac{(H - h_f^{'} - y)^2}{2h_c}\right\}(¥_{sat} - ¥_{unsat}) & \left(H - h_f^{'} < y \le H - h_f^{'} + h_c\right) \\ -(H - y)¥_{unsat} & \left(H - h_f^{'} + h_c < y \le H\right) \end{cases}$$

$$\pm_y{}'(y) = \begin{cases} -(H - h_f^{'} - y)(¥_{sat} - ¥_f) - h_f^{'}\ ¥_{unsat} - \dfrac{h_c}{2}(¥_{sat} - ¥_{unsat}) & \left(0 \le y \le H - h_f^{'}\right) \\ \pm(y) + \dfrac{(H - h_f^{'} + h_c - y)(H - h_f^{'} - y)¥_f}{h_c} & \left(H - h_f^{'} < y \le H - h_f^{'} + h_c\right) \\ -(H - y)¥_{unsat} & \left(H - h_f^{'} + h_c < y \le H\right) \end{cases}$$

Total and effective stress along the y-axis obtained using plane strain, solid and axisymmetric elements are compared with the analytical solution.

Figure 2.22.1
Partially saturated soil model

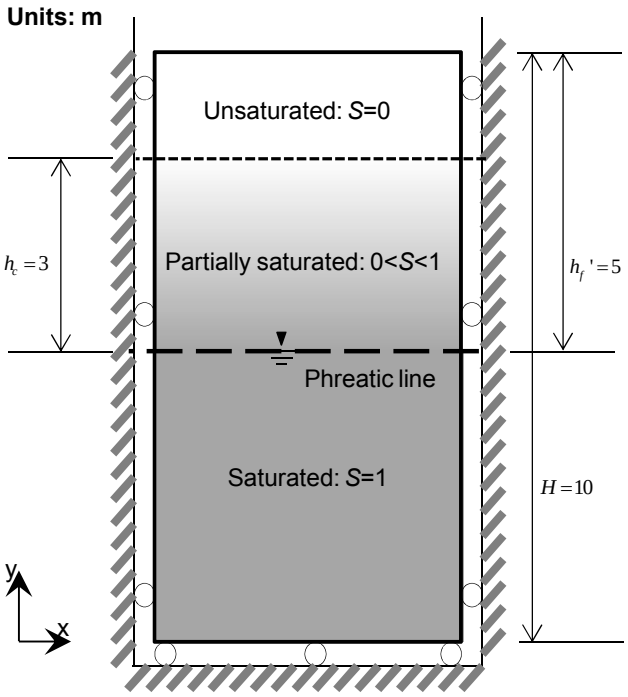

Figure 2.22.2
Effective saturation with respect to pore pressure

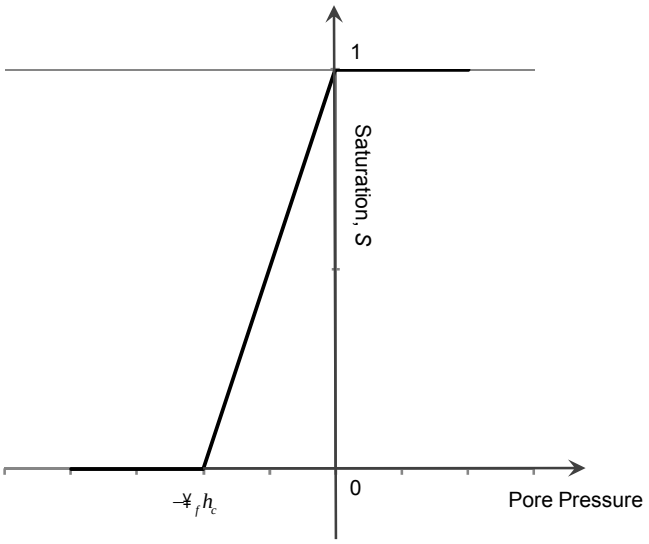

Material data	Young's modulus	*E = 100 kPa*
	Poisson's ratio	¬ *= 0.3*
Weight densities	Water	$¥_f = 9.80665 kN/m^3$
	Saturated soil	$¥_{sat} = 25 kN/m^3$
	Unsaturated soil	$¥_{unsat} = 17 kN/m^3$

Figure 2.22.3
Total and effective vertical stress distributions in partially saturated soil obtained using plane strain elements

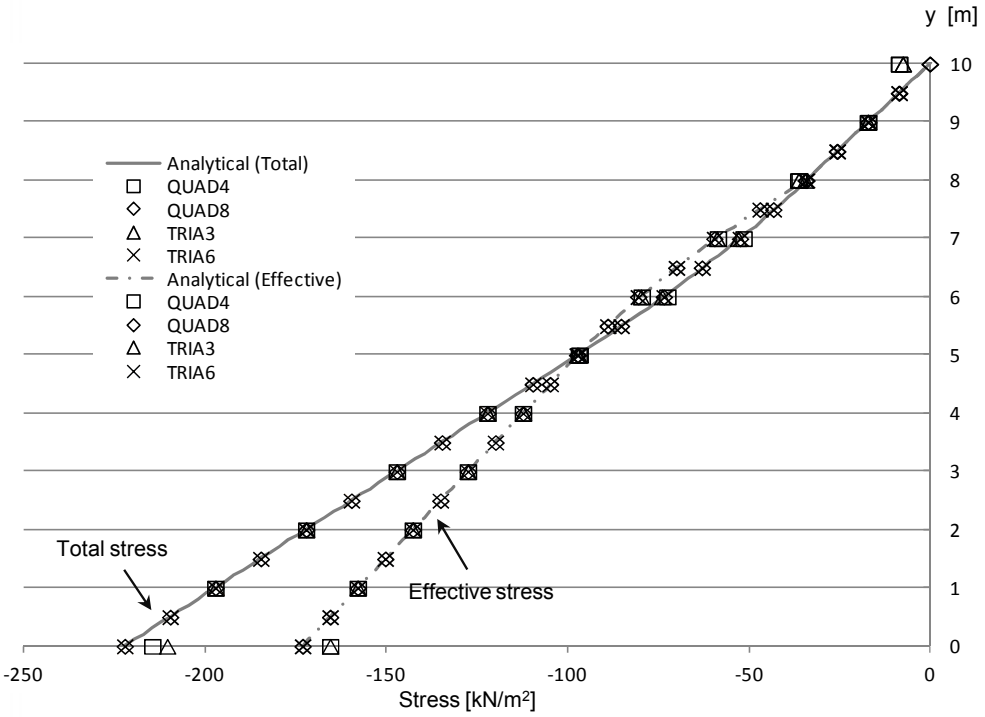

Figure 2.22.4
Total and effective vertical stress distributions in partially saturated soil obtained using solid elements

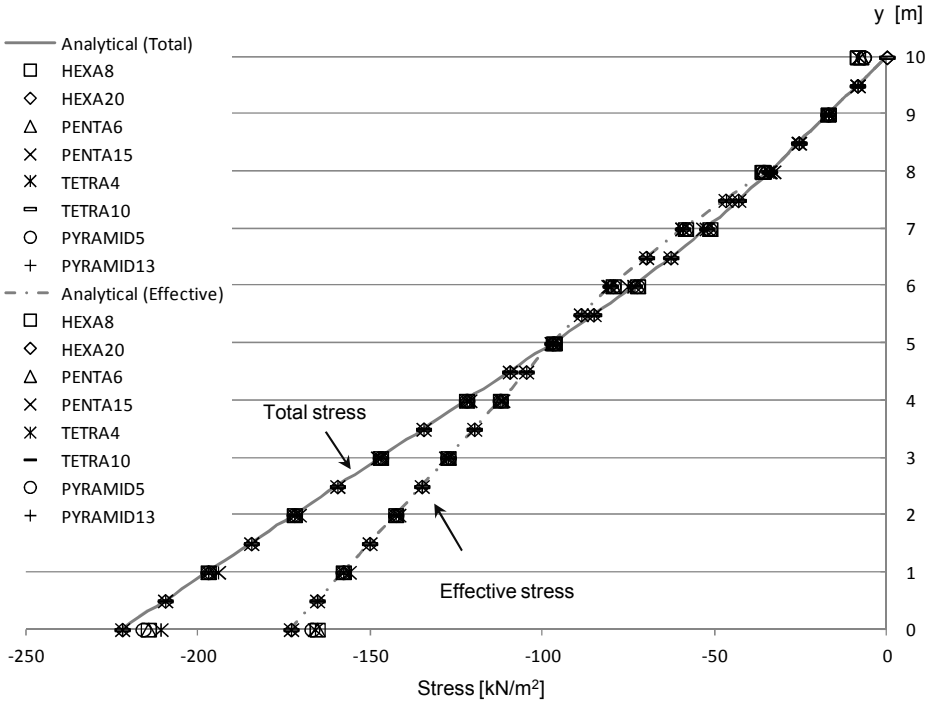

Figure 2.22.5
Total and effective vertical stress distributions in partially saturated soil obtained using axisymmetric elements

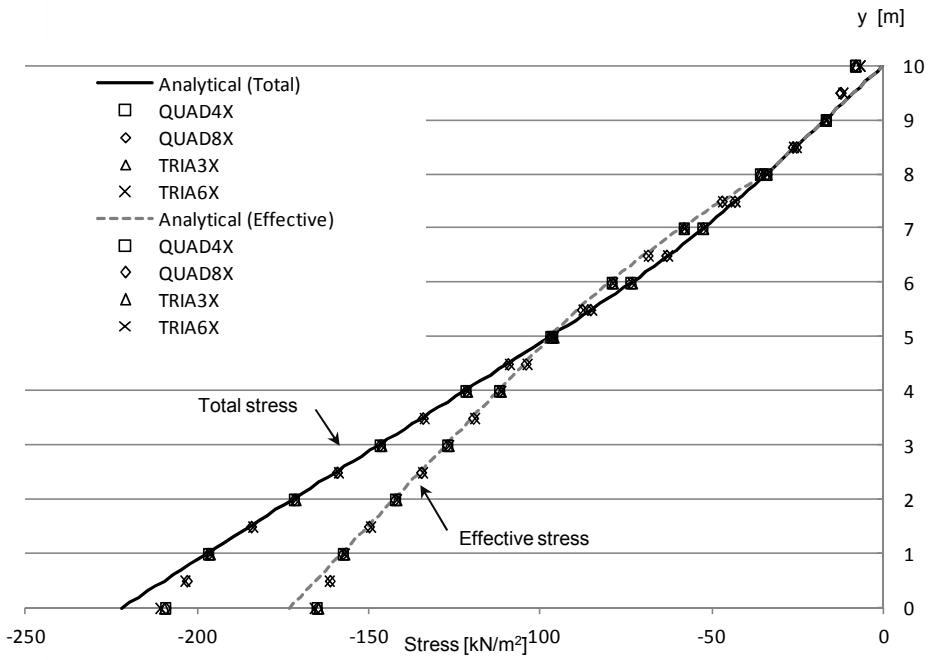

References

1 MacNeal, R.H., and Harder, R.L., "A Proposed Standard Set of Problems to Test Finite Element Accuracy," Finite Element Analysis and Design, Vol. 1, pp. 3-20, 1985

2 Simo, J.C., Fox, D.D., and Rifai, M.S., "On a Stress Resultant Geometrically Exact Shell Model. Part II: The Linear Theory," Computer Methods in Applied Mechanics and Engineering, Vol. 73, pp. 53-92, 1989

3 NAFEMS, "The Standard NAFEMS Benchmarks, Rev. 3", NAFEMS, Glasgow, 1990

4 McCormac, J.C., "Structural Analysis", International Textbook Company, Scranton, PA, 1965

5 Young, W.C., and Budynas, R.G., "Roark's Formulas for Stress and Strain, 7th Edition", McGraw-Hill, New York, 2002

6 Zienkiewicz, O., and XU, Z., "Linked Interpolation for Reisner-Midlin Plate Elements: Part I-A simple quadrilateral," International Journal for Numerical Methods in Engineering, Vol. 36, pp. 3043-3056, 1993

7 Boussinesq, J., "Application des potentials a l'etude de l'equilibre et du movement des solides eastiques", Gauthier-Villars, Paris, 1883

8 Das, B. M., "Fundamentals of Geotechnical Engineering, 2/E", Thomson, 2005